Molecular Degradation of D35 and K77 Sensitizers When Exposed to Temperatures Exceeding 100 °C Investigated by Photoelectron Spectroscopy

Journal:	*Physical Chemistry Chemical Physics*
Manuscript ID	CP-ART-12-2015-007921.R1
Article Type:	Paper
Date Submitted by the Author:	05-Feb-2016
Complete List of Authors:	Oscarsson, Johan; Uppsala University, Department of Physics and Astronomy Fredin, Kristofer; Uppsala University, Department of Physics and Astronomy Ahmadi, Sareh; Uppsala University, Department of Physics and Astronomy Eriksson, Anna; Uppsala University, Chemistry-BMC Johansson, Erik; Uppsala University, Chemistry - Ångström Laboratory Rensmo, Hakan; Uppsala University, Department of Physics and Astronomy

Journal Name

ARTICLE TYPE

Cite this: DOI: 10.1039/xxxxxxxxxx

Molecular Degradation of D35 and K77 Sensitizers When Exposed to Temperatures Exceeding 100 °C Investigated by Photoelectron Spectroscopy

Johan Oscarsson,[a] Kristofer Fredin,[a] Sareh Ahmadi,[a] Anna I. K. Eriksson,[b] Erik M. J. Johansson,[b] and Håkan Rensmo*[a]

Received Date
Accepted Date

DOI: 10.1039/xxxxxxxxxx

www.rsc.org/journalname

Degradation of the materials in dye-sensitized solar cells at elevated temperatures is critical for use in real applications. Both during fabrication of the solar cell and under real working conditions the solar cells will be exposed to heat. In this work, mesoporous TiO_2 electrodes sensitized with the dyes D35 and K77 were subject to heat-treatment and the effects of this were thereafter investigated by photoelectron spectroscopy. For D35 it was found that heat-treatment changes the binding configuration inducing an increased interaction between the sulfur of the linker unit and the TiO_2 surface. The interaction resulting from the change in binding configuration also affects the position of the HOMO level, where a shift of +0.2 eV is observed when heated to 200 °C. For K77, parts of the thiocyanate units are detached and the nitrogen atom leaves the electrode whereas sulfur remains on the surface in various forms of sulfurous oxides. The total dye coverage of K77 gets reduced by heat-treatment. The HOMO level gets progressively less pronounced due to a loss of HOMO level electrons, as a consequence of the lower dye coverage, when heat-treated, which leads to lower excitation rate and lower efficiency. The results are discussed in the context of performance for dye-sensitized solar cells.

1 Introduction

Dye-sensitized solar cells (DSCs) represent a promising technology to harvest the energy emitted by the sun. DSCs are possible to produce in a cost efficient way and they are commonly made from abundant materials. In 1991, the initial DSC paper by O'Regan and Grätzel was published.[1] Since then, a lot of research has been carried out in the field.[2–5] The active part of the cell comprises semiconductor (typically TiO_2) nanoparticles sensitized by a dye for photon absorption and materials used for electron and hole transport (liquid electrolytes or solid state hole conductors). The inner surface area of a mesoporous electrode is far greater than the geometrical area of the sample, which allows for a larger amount of dye molecules to be adsorbed at the surface to absorb more light and generate electrical current.[1,3] The absorption of a photon, promotes electron excitation in the dye and subsequent transfer to the TiO_2 nanoparticle from which the electron is conducted through the TiO_2 matrix to the back contact. In a similar way the remaining hole is transferred to the electrolyte or hole conductor, which fills up the pores, and transported to the counter electrode. Solar cells relying on this principle and utilizing liquid electrolyte as hole conducting medium have shown high power conversion efficiencies (12 - 14 %)[6–8] whereas the efficiency for devices incorporating solid or polymer materials (solid state DSCs, ssDSCs) is slightly lower.[9–11]

Dye-sensitized working electrodes and complete DSC devices are frequently exposed to elevated temperatures. Liquid DSCs use a thermoplastic to assemble the working and counter electrodes. Normally, the thermoplastic requires temperatures in the range of 100-130 °C for sealing the electrodes together.[12–14] One method to prepare ssDSCs includes infiltration of a hole conductor in its molten form into the sensitized TiO_2 electrode,[15] which offers the advantage of utilizing thicker TiO_2 and still obtain efficient pore filling. Target areas for solar cell use may be remote locations off the normal grid with extreme weather conditions, resulting in very warm solar cells during operation. Under most conditions, the internal operating temperature of the solar cells is around 40-50 °C, but in extreme weather conditions it can reach up to 70 °C.[16,17] The effect of heat-treatment has gained attention when it was showed that the performance of DSCs comprising pre heat-treated working electrodes was lower than that of the pristine counterpart.[18–23]

Historically (and still), dyes based on Ruthenium have given highly efficient solar cells.[24–29] Many organic dyes exist today

[a] Department of Physics and Astronomy, Uppsala University, Box 516, SE-75120 Uppsala, Sweden. E-mail: hakan.rensmo@physics.uu.se
[b] Department of Chemistry-Ångström, Uppsala University, Box 523, SE-75120 Uppsala, Sweden.

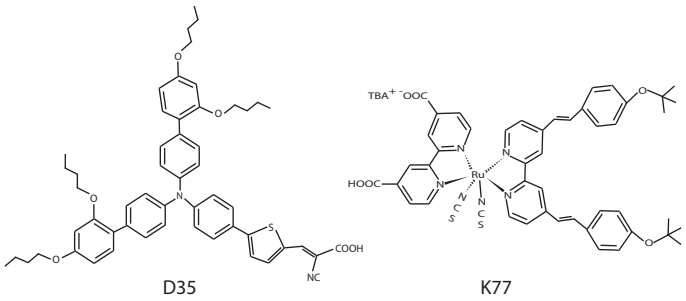

Fig. 1 Chemical structures of the dye molecules D35 (left) and K77 (right).

and many of them also give high efficiencies.[28–32] Herein the effects of heat-treatment on two dye sensitizers; the organic D35[33] (based on the D5 dye[34] with additional ligands) and K77[35] (from the N3[36] family with additional ligands) are investigated; see their respective molecular structures in Figure 1. The study comprises both measurements on the molecular scale where pre-heat-treated dye-sensitized working electrodes are examined using photoelectron spectroscopy (PES) as well as on the performance of DSCs comprising such electrodes.

2 Experimental

2.1 Sample preparation

Plates of conducting glass (Pilkington TEC8) were cleaned for 1 hour in a detergent solution, water and finally in ethanol in an ultrasonic bath.[37] Clean substrates for working electrodes were immersed in an aqueous 40 mM $TiCl_4$ solution at 70 °C for 1.5 hours. Electrodes used for absorbance and photoelectron spectroscopy (PES) measurements were prepared by screen-printing 5x5 mm^2 single layers of TiO_2 paste (Solaronix T37/SP) onto the substrates, giving 5 μm thick TiO_2 films. Working electrodes used in all other measurements were prepared by screen-printing two layers of TiO_2 followed by two layers of light scattering TiO_2 paste (Solaronix D/SP), with a film thickness of 10 μm (plus 3 μm scattering layer). The electrodes were sintered in an oven (Nabertherm Controller P320) on a four level temperature gradient program; 180 °C (10 min), 320 °C (10 min), 390 °C (10 min) and 500 °C (60 min).[33]

Cleaned conducting glass substrates used for counter electrodes were covered with a solution containing 4.8 mM H_2PtCl_6 in ethanol (10 μlcm^{-2}) and left to dry. They were sintered in an oven set at 350 °C for 30 minutes and thereafter left in the oven to cool down.

A K77 dye solution was prepared by dissolving 0.3 mM Ru(2,2'-bipyridine-4,4'-dicarboxylic acid)(4,4'-bis(2-(4-*tert*-butyloxyphenyl)ethenyl)-2,2-bipyridine)$(NCS)_2$ in a 1:1 volumetric mixture of *tert*-butanol and acetonitrile. A D35 dye solution was prepared by dissolving 0.3 mM (E)-3-(5-(4-(bis(2',4'-dibutoxybiphenyl-4-yl)amino)phenyl)thiophen-2-yl)-2-cyanoacrylic acid in 99 % ethanol. The dye load for samples used for absorbance measurements was controlled by their time in the dye solution; 30 seconds for samples sensitized with D35 and 10 minutes for samples sensitized with K77. Samples prepared for other measurements were immersed in the solution overnight, approximately 12 hours.

Heat-treated working electrodes were prepared by placing dye-sensitized electrodes on a pre-heated hotplate (IKA C-MAG HP7) set at 100, 150 or 200 °C for a duration of 5 minutes in ambient air conditions (measurements performed in a lab in air at 1 atm., in a temperature of 20 °C and a humidity between 40-50 %). Pristine electrodes used in the study as references were not subject to this.

The electrolyte was prepared by dissolving 1.0 M 1-butyl-3-methylimidazolium iodide, 30 mM I_2, 0.10 M guanidine thiocyanate and 0.50 M *tert*-butylpyridine in a 3:1 volumetric mixture of acetonitrile/valeronitrile.

Solar cells were prepared by assembling the working electrodes with the counter electrodes using Surlyn films (30 μm thickness) as spacer and clips to assure that the distance between the respective electrodes did not exceed the thickness of the spacer. Clips were used to fully control the heat-treatment of the electrodes. Fast drying glue was used to assure complete sealing and mechanical stability and finally the electrolyte was introduced through pre-drilled holes in the counter electrode.

The dyes used are good representatives of both organic and inorganic dyes. Neither the thickness of the TiO_2 films nor the electrolyte composition were optimized for the different dyes. This means that the power conversion efficiency of the pristine samples could have been higher. However, the aim was to study the effect of heat-treatment, which still can be done in a good way in these two simple and well-defined systems.

2.2 Photoelectron Spectroscopy measurements

Photoelectron spectroscopy (PES) is because of its high surface sensitivity and element specificity a powerful tool for studying interfaces in DSCs.[4] The properties of the TiO_2/dye interfaces were studied using synchrotron based PES at the undulator beamline I411[38,39] at the Swedish national synchrotron facility MAX-IV in Lund. The electron take off angle was 70 ° and the electron take off direction was collinear with the e-vector of the incident photon beam, *i.e.* the analyzer was placed orthogonal to the incoming photon beam. A Scienta R4000 WAL analyzer was used to measure kinetic energies of ejected photoelectrons. All measured spectra were energy calibrated versus the $Ti2p_{3/2}$ peak, which was set to a binding energy of 458.56 eV.[40] Intensity referencing was done with respect to the $Ti2p_{3/2}$ peak. To prevent radiation damage, the samples were moved regularly. Radiation damage on each spot was monitored through repeated measurements. No signs of radiation damage were observed in the measurements reported below.

2.3 Solar cell characterization

Absorbance measurements of dye-sensitized TiO_2 films were done using an absorption spectrometer (Ocean optics HR2000) with a Mikropack DH-2000-BAL light source. All measurements were corrected for light scattering by subtracting the absorbance of the un-sensitized TiO_2 film.

The current-voltage (IV) characteristics of the solar cells were

studied using a Keithley 2400 source/meter and a solar simulator (Newport 91160). The light intensity was calibrated to 1000 Wm^{-2} (1 sun) using a certified reference solar cell (Fraunhofer ISE). A black mask of 5x5 mm^2 was used during the IV-measurements to avoid additional contribution from light hitting outside of the active area of the solar cell.

Electron lifetime measurements were conducted in a darkened cabinet, the "tool-box", using a white LED (Luxeon Star 1 W) as light source. A 16-bit digital acquisition board (National Instruments) was used in combination with a current amplifier (Stanford Research Systems SR570) and a custom-made system using electromagnetic relay switches to record current and voltage. The electron lifetime, τ_e, which depends on the recombination dynamics can be calculated from the amount of charge stored in the device divided by the recombination current; a ratio that can be calculated through a voltage decay experiment provided that the charge-voltage relation, $Q_{OC}(V_{OC})$, is known. Accordingly, the charge stored in the samples during open-circuit, Q_{OC}, was measured with respect to the open-circuit voltage, V_{OC}, for all samples where V_{OC} was controlled by using various light intensities. It was found that however the values of V_{OC} were lower for the pre-heated samples the relation $Q_{OC}(V_{OC})$ was similar. The voltage decay was then measured for all samples by turning off the light source and the values of τ_e calculated according to $\tau_e = Q_{OC}/\frac{dQ_{OC}}{dt}$ where the values of Q_{OC} were obtained through the $Q_{OC}(V_{OC})$ relation and the derivative calculated from the slope of the decay.[41]

3 Results and discussion

3.1 Photoelectron spectroscopy measurements

3.1.1 Molecular surface structure for D35.

In Figure 2, the N1s spectra of the D35 samples are shown (overview spectra of the D35 samples with peak assignments are shown in Figure S1 in Supporting Information). There are two chemically inequivalent nitrogen atoms present in D35, N_D and N_A, where the indices refer to the donor (TAA) and acceptor (CN) units respectively. The N1s core level spectra consist of two separate parts. The peak at 399.3 eV is ascribed to N_D whereas the peak at 398.4 eV correspondingly is ascribed to N_A.[42]

Figure 3 shows the S2p spectra for the D35 samples. D35 has a single sulfur atom in the structure. However, the S2p core level spectra clearly consist of two components and two sets of spin-orbit split peaks are needed for de-convolution. The two doublets are separated by approximately 0.75 eV, which is comparable to what has been observed for similar dyes earlier.[43] The doublet with the largest intensity is referred to as S_L where the index refers to the linker unit, while the doublet with lower intensity is referred to as S_E, where E is for Extra. The presence of S_E can, as for metalorganic dyes[40], be explained by a mixture of binding geometries. For D35 (and similar dyes) S_L is attributed to the dye adsorbing to the TiO_2 standing on the surface while S_E is from the dye adsorbing with a large angle (almost lying on the TiO_2 surface) to the surface normal.[43] The latter configuration allows interaction between the sulfur in the dye and the TiO_2 surface placing the sulfur in a different chemical environment which leads to the large chemical shift observed.

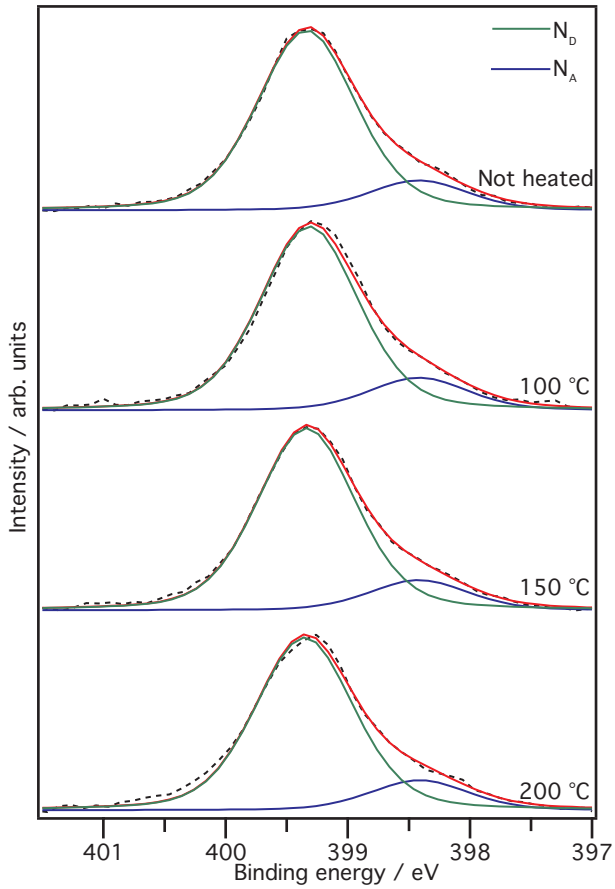

Fig. 2 N1s spectra of the D35 samples measured with a photon energy of 535 eV.

A thorough analysis of the N1s data shows no change in the N_A to N_D ratio for pre-heated samples as compared to the pristine sample, see Table 1. For sulfur however the ratio S_E to S_L is double the value for the sample pre-heat-treated at 200 °C in comparison to the pristine sample. A quantification reveals a decrease in the amount of S_L from 91 % (pristine) to 83 % (200 °C) of the total sulfur signal.

The relative amounts of nitrogen and sulfur in D35 with respect to titanium were quantified through the relative intensities of N1s and S2p with respect to $Ti2p_{3/2}$. This procedure gives an estimation of the amount of sulfur and nitrogen relative to the amount of titanium, *i.e.* it provides an estimation of the surface coverage. The ratios are presented in Table 1. No significant change resulting from heat-treatment is observed, which implies that no parts of the dye molecules comes loose from the heat-treatment.

Table 1 Intensity ratios from PES measurements of the D35 samples

	Not heated	100 °C	150 °C	200 °C
$\frac{N1s}{Ti2p}$	0.93	1.06	0.94	1.04
$\frac{S2p}{Ti2p}$	0.55	0.65	0.53	0.58
$\frac{N_A}{N_D}$	0.17	0.18	0.17	0.17
$\frac{S_E}{S_L}$	0.10	0.11	0.12	0.20
$\frac{S_L}{S2p}$	0.91	0.90	0.89	0.83

The valence electronic structure is important for the charge

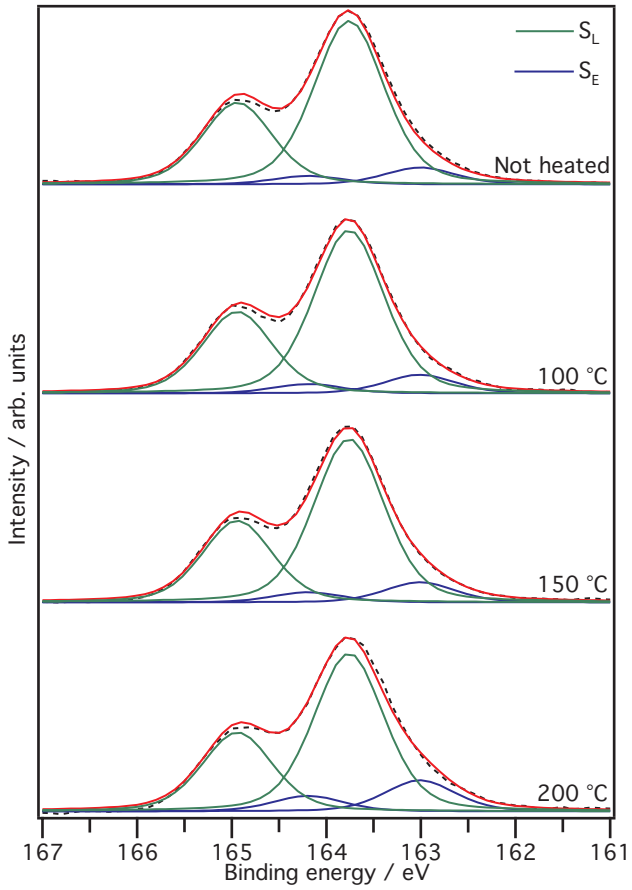

Fig. 3 S2p spectra of the D35 samples measured with a photon energy of 454 eV.

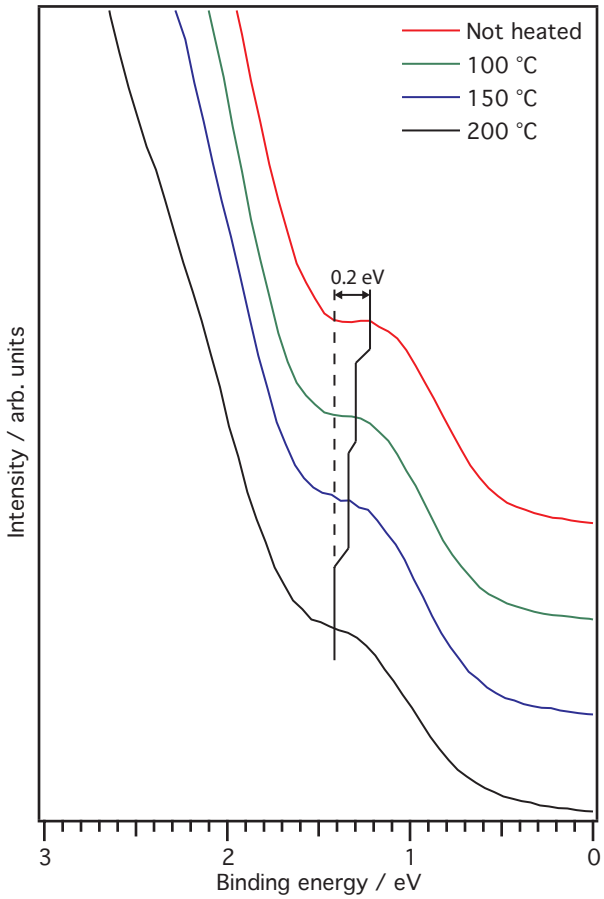

Fig. 4 Valence spectra of the D35 samples measured with a photon energy of 100 eV. The connected vertical lines show the position of the HOMO peak in the samples. A shift of +0.2 eV is indicated by the arrow.

transfer processes in the solar cells, and changes in this region therefore have direct influence on the device properties. The outermost parts of the valence region (HOMO levels) are shown in Figure 4 for the D35 samples. It can be observed that the HOMO level becomes progressively less pronounced for the heat-treated samples. A clear difference can be seen between the pristine sample and the heat-treated samples.

From Figure 4 we observe that the HOMO-level in D35 shifts towards higher binding energy when heat-treated, as indicated by the connected vertical lines in the figure. Comparing the sample heat-treated at 200 °C to the pristine sample reveals a shift of the HOMO peak of 0.2 eV, while the samples heat-treated at 100 and 150 °C show shifts of 0.1 and 0.13 eV respectively. This suggests that two species are present at the surface when D35 is used and that heat-treatment alters the relative ratio between them (as also seen by the increase upon heat-treatment of the S_E component in the S2p spectra in Figure 3). These two species can be ascribed to two different binding configurations. The HOMO of D35 is predominantly located at the donor part of the molecule (TAA) with contributions from the phenyl groups with the alkoxy chains.[33,44] This is in agreement with what has been observed for the HOMO of TAA dyes previously.[45,46] As seen previously D35 adsorbs predominantly to TiO_2 standing up.[43,44] Heat-treatment will cause

a change in binding configuration of some of the D35 molecules. The change in binding configuration affects the bridging and anchoring parts of the molecule since the sulfur spectra show clear evidence of interaction with the TiO_2. When the binding configuration changes, the binding angle of D35 to the normal of TiO_2 changes. By that, an interaction between the donor part of the molecule and the TiO_2 surface (via the alkoxy chains of D35) also can take place. Since the HOMO is located on the TAA and on the phenyl groups this interaction should also induce a shift of the HOMO level, which is also observed.

At this point it is important to note that not only changes in energy matching (Figure 4) can have important effects on the overall solar cell performance. Small variations in surface binding configurations where the TAA is close to the TiO_2 surface will facilitate charge recombination and might have substantial effects on the conversion process.

3.1.2 Molecular surface structure for K77.

K77 contains seven nitrogen atoms including the cation unit. There are four nitrogen atoms in the bi-pyridine unit, two in the thiocyanate unit and one in the *tert*-butyl ammonium (TBA) cation unit. Thus, there are three chemically inequivalent types of nitrogen atoms in K77. Figure S2 in Supporting Information, shows the overview spectra of the K77 samples with the corresponding peak assignments. Figure 5 shows the N1s core level spectra for the K77 samples. From the spectra it can be seen that four components are necessary for de-convolution. The thiocyanate groups often give rise to two nitrogen peaks and two sulfur spin-orbit split doublets when interacting with a TiO_2 surface.[40,47] The peaks are referred to as: N_P for the bipyridine nitrogen, N_{NCS1} and N_{NCS2} for the thiocyanate nitrogens and N_{TBA} for the TBA nitrogen. The peaks at the lowest binding energies at 397 and 398.1 eV, see Figure 5, originate from the thiocyanate units, the large peak at 399.8 eV from the bipyridine units and the small peak at 402 eV from the TBA cation.[40] The difference in energy for the peaks assigned to the thiocyanate nitrogens suggests that part of the thiocyanate nitrogens have a different chemical surrounding, which is caused by interactions with the TiO_2 surface.

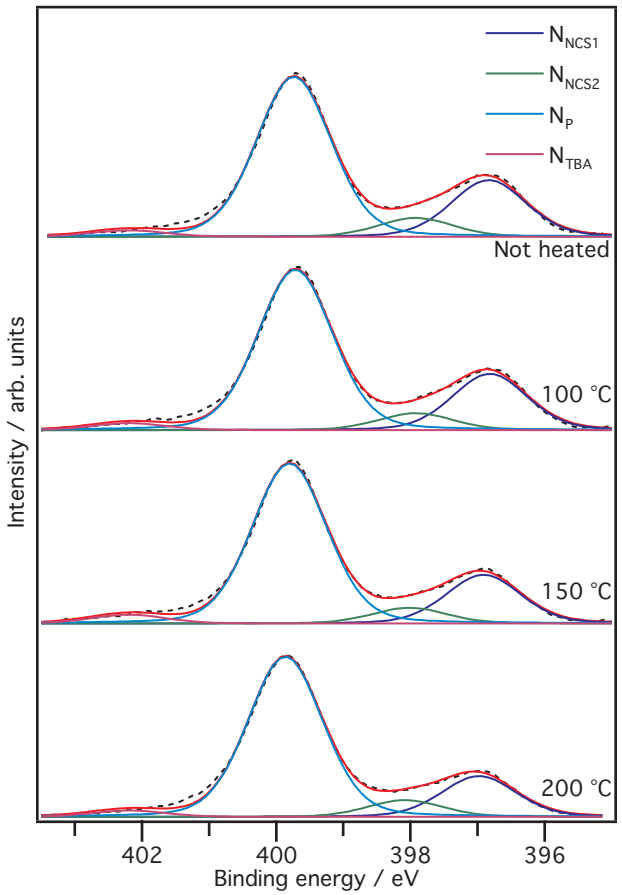

Fig. 5 N1s spectra of the K77 samples measured with a photon energy of 535 eV.

The S2p core level spectra are displayed in Figure 6. Five spin-orbit split doublets were used to de-convolute the data. The sulfur atoms from the thiocyanate units are accordingly referred to as S_{NCS1} and S_{NCS2} and are assigned to the doublets with the lowest binding energies.[40,47] In a similar way as the thiocyanate nitrogen, the multiple peaks for the thiocyanate sulfurs suggest that the atoms to some extent interact with the TiO_2 surface. The doublets at higher binding energies originate from various compositions of sulfurous oxides; the contribution at around 168 eV is attributed to SO_4 and the one at 166.5 eV to SO_3 and they are hereafter referred to as S_{SO_4} and S_{SO_3} respectively. The positions of the components are in agreement with previously reported positions for sulphates at metal and metal oxide surfaces.[48–51] The nature of the contribution at 164 eV is unclear and is therefore referenced to as S_{SO_X}. The relative amounts of nitrogen and sulfur with respect to titanium were estimated through the relative intensities of N1s and S2p with respect to $Ti2p_{3/2}$, see the results in Table 2.

In contrast to what was measured for nitrogen present in D35, the relative amount of nitrogen with respect to titanium decreases progressively with increasing heating temperature for samples sensitized with K77. The relative contribution from N_{TBA} to the total N1s signal remain constant at around 3 % for all samples, whereas the relative contributions from N_{NCS1} and N_{NCS2} de-

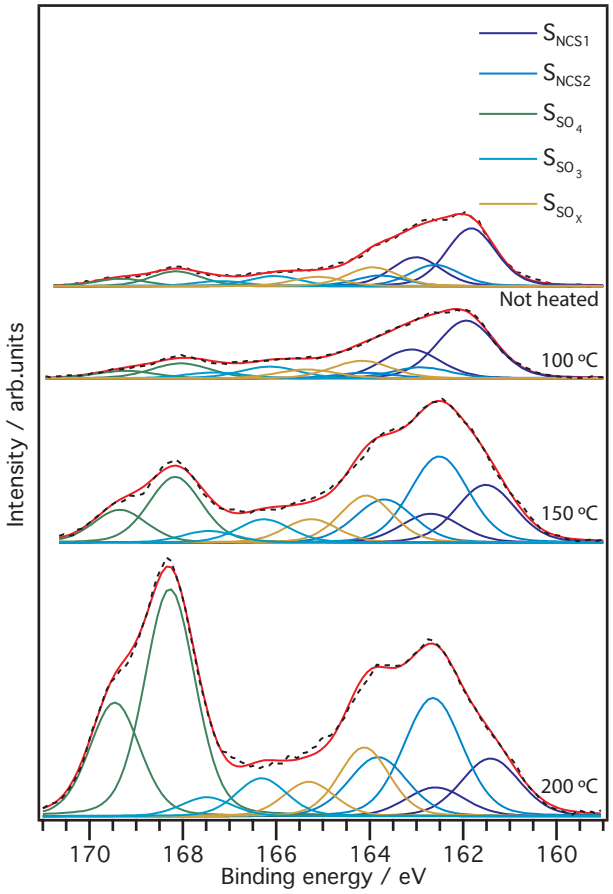

Fig. 6 S2p spectra of the K77 samples measured with a photon energy of 454 eV.

Table 2 Intensity ratios from PES measurements of the K77 samples

	Not heated	100 °C	150 °C	200 °C
$\frac{N1s}{Ti2p}$	1.44	1.26	0.96	0.92
$\frac{S2p}{Ti2p}$	0.20	0.20	0.21	0.22
$\frac{N_P}{N1s}$	0.66	0.67	0.68	0.70
$\frac{N_{NCS}}{N1s}$	0.31	0.30	0.28	0.25

crease from 31 to 25 % when comparing the pristine sample with the sample pre-heat-treated at 200 °C. This suggests that the relative amount of N_P remains constant as the decreasing ratio of N_{NCS} and N_P which is consistent with the decreasing ratio of N1s with respect to Ti2p. The amounts of sulfur from the thiocyanate units, S_{NCS1} and S_{NCS2}, are basically half that of the pristine value for samples pre-heat-treated at 200 °C. At the same time the contribution from various compositions of sulfurous oxides is almost a factor of three larger for samples pre-heat-treated at 200 °C while the relative ratio of sulfur versus titanium remains constant. Consequently, the peaks at higher binding energies are assessed to sulfurous compounds created during the heat-treatment process.

The combined data for N1s and S2p indicate that a part of the thiocyanate units, -NCS, is detached from the K77 molecule when it is subject to elevated temperatures. Possible reactions that are consistent with the data are that nitrogen from -NCS leaves the system in the form of NO_X or N_2 whereas sulfur on the other hand oxidizes and binds to the TiO_2 surface as SO_X.

Figure 7 shows the C1s and $Ru3d_{5/2}$ levels of the K77 samples. A clear decrease in signal as a function of heating temperature is observed both for C1s and Ru3d. A quantification of the decrease was done by comparing the areas of the peaks. Normalizing the pristine C1s peak to 1 gives areas of 0.87, 0.73 and 0.56 for the samples heat-treated at 100, 150 and 200 °C respectively. The $Ru3d_{5/2}$ peak gave areas of 1, 0.79, 0.72 and 0.66 for the pristine sample, samples heat-treated at 100, 150 and 200 °C respectively. As seen the ratios for C1s and Ru3d agrees quite well. The reason for the small difference between them can be ascribed to the presence of small amounts of surface adsorbed carbon, which is expected on ex-situ samples. However, the overall trend is the same. This trend together with the loss of nitrogen from heat-treatment indicates that part of the K77 molecules detach from the TiO_2 when heated, *i.e.* the dye coverage decreases with increasing temperature. However, as seen from the S2p spectra presented in Figure 6, sulfur remains on the TiO_2 surface in various forms of sulfurous oxides.

The outermost part of the valence region of K77 is shown in Figure 8. No difference in binding energy of the HOMO level can be detected due to the heat-treatment, which to some extent can be expected considering that the HOMO-level is predominantly located on the ruthenium atom[52] and therefore quite stable. However, the HOMO peak becomes slightly less pronounced and in turn broader with increasing heating temperature. This means that there are fewer electrons at the HOMO level in the heat-treated samples as compared to the pristine reference sample, as indicated by the Ru3d spectra presented in Figure 7. Since the HOMO level mostly consist of Ru4d electrons[52], the loss of HOMO level electrons is ascribed to the lower dye cov-

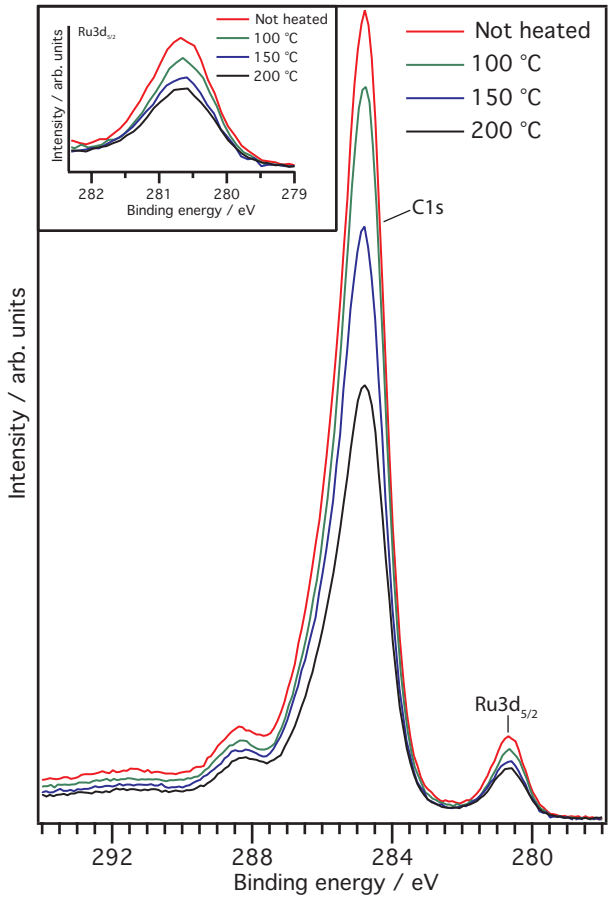

Fig. 7 C1s and Ru3d spectra of the K77 samples measured with a photon energy of 758 eV. The inset shows a magnification of the $Ru3d_{5/2}$ core level.

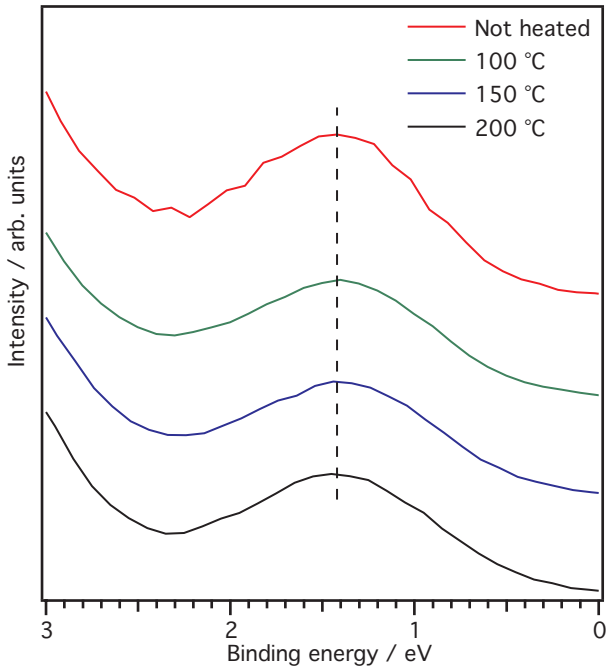

Fig. 8 Valence spectra of the K77 samples measured with a photon energy of 454 eV. The dashed line indicates the position of the HOMO level in all samples.

erage of K77 (molecular desorption and dissociation) from heat-treatment. To quantify how much fewer electrons there are at the HOMO level after heat-treatment a comparison of the area of the HOMO peaks was done. The area of the pristine HOMO peak was normalized to 1, giving areas of 0.72, 0.69 and 0.63 for the samples heat-treated at 100, 150 and 200 °C respectively. This is in agreement with what was found for the Ru3d peaks. Heat-treatment thus affect the HOMO level which in turn means that the rate of excitation of K77 will be lower for heat-treated samples. This can be one of the reasons leading to a lower overall efficiency of the heat-treated cells.

3.2 Absorbance measurements

To elucidate the influence of heat-treatment on the electrodes' ability to harvest photons, the absorbance (A) was measured before and after heat-treatment. The difference in absorbance, ΔA, between the heat-treated and the pristine samples can be viewed in Figures 9 and 10 for samples sensitized with D35 and K77 respectively, with the absorbance of the pristine samples as insets. In Figure 9 it can be observed that around 400 nm, there is a slight increase in absorbance for pre heat-treated samples and this effect increases with temperature. In contrast, for values of λ between 420 and 600 nm, there is a pronounced decrease in absorbance, also with a magnitude determined by the heating temperature. An isosbestic point at $\lambda \approx 425$ nm indicates that only two molecular species absorb in that region and, consequently, that only one product is formed during heat-treatment for D35. This agrees with the results obtained from the photoelectron spectroscopy measurements, which also suggest two different species ascribed to different adsorption geometries. In

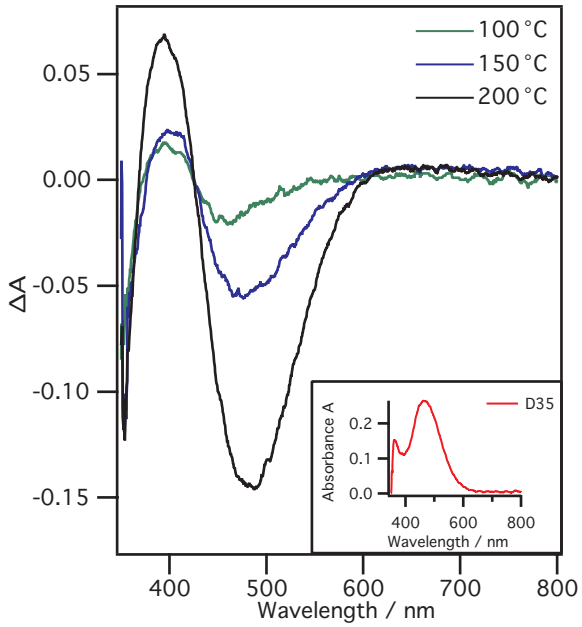

Fig. 9 Difference in absorbance (ΔA) for the D35 samples. Absorbance of the pristine D35 sample in inset.

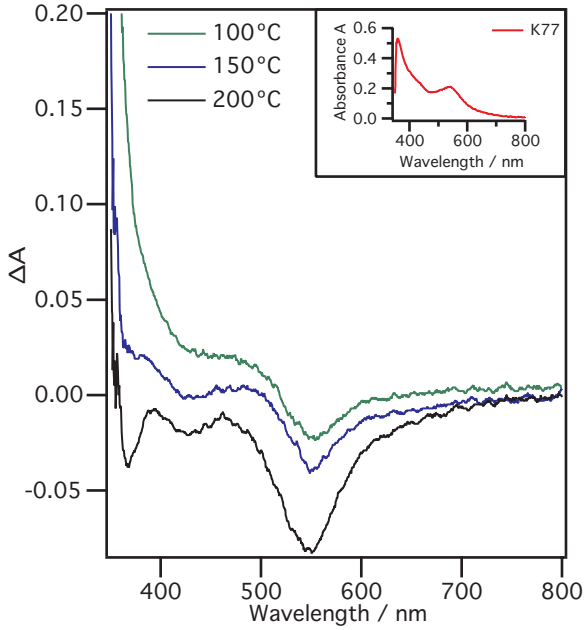

Fig. 10 Difference in absorbance (ΔA) for the K77 samples. Absorbance of the pristine K77 sample in inset.

Figure 10, which depicts the difference in absorbance for electrodes sensitized with K77, the absorbance increases at shorter wavelengths, whereas it decreases for longer wavelengths. The absence of an isosbestic point indicates that multiple products are formed by heat-treatment of electrodes sensitized with K77. This also agrees with the photoelectron spectroscopy results, suggesting several products obtained after heat-treatment.

From the absorbance measurements can be concluded that heat-treatment has a negative impact on the cells' ability to absorb photons at longer wavelengths, which agree with the PES measurements of the HOMO levels, see Figures 4 and 8. This will affect the solar cell performance negatively and below we show the results for the solar cell performance after the heat-treatment.

3.3 Influence of heat-treatment on devices

The influence of heat-treatment on the performance of model DSC devices was measured and it was found that the respective power conversion efficiency, η, was significantly lower for the samples comprising pre-heated electrodes. We use the same type of thin electrodes as above to enable direct comparison of the results from the surface investigations, although the performance is lower compared to a thicker optimized device. The values of η were 4.4 and 4.5 % for the pristine samples sensitized with D35 and K77 respectively, which were slightly reduced to 4.0 % for both sensitizers while utilizing working electrodes pre heat-treated at 100 °C. The efficiency decreases strongly with an increasing pre heat-treatment temperature; for samples heat-treated at 150 °C the efficiency is 2.3 and 1.8 % respectively and for 200 °C it is 0.1 and 0.3 %. The spectral response (IPCE not shown) showed a general decrease in the IPCE. As expected from the absorbance data (Figure 9 and 10), the decrease was more pronounced at longer wavelengths. A summary of all solar cell characteristics can be seen in Tables 3 and 4 for D35 and K77 respectively. The lower efficiencies recorded for pre-heat-treated samples are mainly due to a strongly reduced short-circuit current, j_{SC}, which drops from around 8 to 9 mAcm^{-2} for the pristine samples to about 1 mAcm^{-2} for samples heat-treated at 200 °C. To some extent also lower values of the open-circuit voltages, V_{OC}, contribute to the effect; the values of V_{OC} drop from around 0.8 V to about 0.5 V for the heat-treated samples. However, a lower absorbance explains the reductions in both j_{SC} and V_{OC}. The alterations in the dyes' molecular structure may also have an influence on the back reaction processes. These recombination processes may severely decrease the performance for heat-treated samples if the dyes' ability to shield and separate the respective charge is lowered as a result of molecular re-arrangements at the TiO_2/dye interface. To investigate the recombination processes, the electron life time, τ_e, in the solar cells was estimated from the photovoltage change upon a small modulation of the excitation light.[41] The values of τ_e can be viewed with respect to V_{OC} in Figures 11 and 12 for samples sensitized with D35 and K77 respectively. As shown, τ_e decrease progressively with V_{OC} and pre-heat-treatment temperatures, which implies that recombination is faster in pre-heat-treated samples. In the figures it can also be seen that the values of τ_e are higher for samples sensitized with D35 than K77 indicating that samples sensitized with D35 inhibit recombination more efficiently than K77.

Table 3 Summary of solar cell characteristics of the D35 samples

	Not heated	100 °C	150 °C	200 °C
V_{OC} (V)	0.85	0.84	0.78	0.48
J_{SC} $(mAcm^{-2})$	8.09	7.20	4.45	0.22
FF	0.64	0.65	0.66	0.56
η (%)	4.4	4.0	2.3	0.1

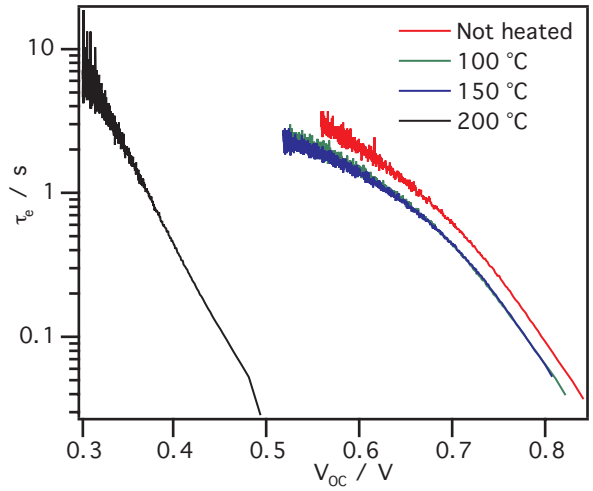

Fig. 11 Electron lifetimes of the D35 samples.

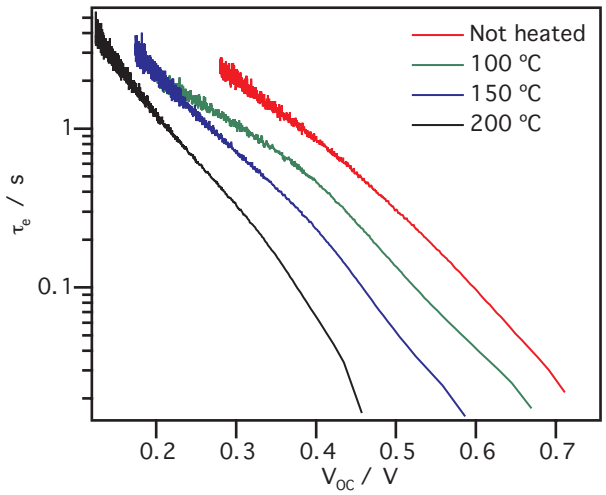

Fig. 12 Electron lifetimes of the K77 samples.

Table 4 Summary of solar cell characteristics of the K77 samples

	Not heated	100 °C	150 °C	200 °C
V_{OC} (V)	0.72	0.69	0.62	0.50
J_{SC} $(mAcm^{-2})$	9.25	8.19	4.21	0.95
FF	0.68	0.70	0.68	0.66
η (%)	4.5	4.0	1.8	0.3

It is noteworthy that the power conversion efficiency of D35 drops by 98 % when heat-treated at 200 °C as compared to the pristine sample, even though all dye molecules still remain on the surface. It is an even bigger efficiency loss than for K77 (93 %) where the dye molecules actually dissociate and partly desorb from the heat-treatment. Thus, binding configurations of the dye on the TiO_2 surface is of great importance for the function of the entire solar cell.

4 Conclusions

Mesoporous electrodes sensitized with the dyes D35 and K77 were subject to heat-treatment and the molecular compositions were thereafter investigated by photoelectron spectroscopy. For D35 it was found that heat-treatment changes the sulfur unit in the dyes' linker unit, due to a different dye configuration on the TiO_2 surface. The valence electronic structure of the dye changes as a consequence of heat-treatment. A shift of the HOMO level of +0.2 eV is observed for the sample heat-treated at 200 °C. This leads to an increase of the HOMO-LUMO gap, which is also observed in the light absorbance spectra, which gives a lower photon absorption in the heated electrodes, causing a decrease in conversion efficieny. For K77, parts of the thiocyanate units are detached (molecular dissociation) and the nitrogen atom leaves the electrode whereas sulfur remains on the surface in various forms of sulfurous oxides. In addition, the dye coverage of K77 decreases as a consequence of heat-treatment. In the valence electronic structure, the HOMO level gets less pronounced with increasing heating temperature. The loss of HOMO level electrons due to heat-treatment is ascribed to lower dye coverage, with lower absorption rate and overall efficiency as a consequence, which was also observed in the light absorbance spectra. It was found that the performance of the devices was dramatically reduced after heat-treatment and that the major loss was due to a strongly reduced current density. This was traced to a strongly reduced absorbance for longer wavelengths in combination with an increased rate of the back reaction for pre-heated samples. We conclude that in the struggle to tailor the design for efficient dye-sensitized solar cells, the effect of heat-treatment should be considered as samples may be exposed to this condition during preparation and due to environmental factors.

5 Acknowledgements

The kind and helpful staff at the MAX-IV laboratory is greatly acknowledged. This work was funded by the Swedish Energy Agency, the Swedish Research Council FORMAS, and the Swedish Research Council (VR).

References

1 B. O'Regan and M. Grätzel, *Nature*, 1991, **353**, 737–740.

2 L. M. Peter, *Phys. Chem. Chem. Phys.*, 2007, **9**, 2630–2642.

3 A. Hagfeldt, G. Boschloo, L. Sun, L. Kloo and H. Pettersson, *Chem. Rev.*, 2010, **110**, 6595–6663.

4 E. M. J. Johansson, R. Lindblad, H. Siegbahn, A. Hagfeldt and H. Rensmo, *ChemPhysChem*, 2014, 1006–1017.

5 J. Albero, P. Atienzar, A. Corma and H. Garcia, *The Chemical Record*, 2015, **15**, 803–828.

6 A. Yella, H.-W. Lee, H. N. Tsao, C. Yi, A. K. Chandiran, M. Nazeeruddin, E. W.-G. Diau, C.-Y. Yeh, S. M. Zakeeruddin and M. Grätzel, *Science*, 2011, **334**, 629–634.

7 S. Mathew, A. Yella, P. Gao, R. Humphry-Baker, B. F. E. Curchod, N. Ashari-Astani, I. Tavernelli, U. Rothlisberger, M. K. Nazeeruddin and M. Grätzel, *Nature chemistry*, 2014, **6**, 242–7.

8 K. Kakiage, Y. Aoyama, T. Yano, K. Oya, J.-i. Fujisawa and M. Hanaya, *Chem. Commun.*, 2015, **51**, 15894–15897.

9 N. Cai, S. J. Moon, L. Cevey-Ha, T. Moehl, R. Humphry-Baker, P. Wang, S. M. Zakeeruddin and M. Grätzel, *Nano Letters*, 2011, **11**, 1452–1456.

10 X. Liu, W. Zhang, S. Uchida, L. Cai, B. Liu and S. Ramakrishna, *Advanced Materials*, 2010, **22**, 150–155.

11 J. Burschka, A. Dualeh, F. Kessler, E. Baranoff, N.-L. Cevey-Ha, C. Yi, M. K. Nazeeruddin and M. Grätzel, *Journal of the American Chemical Society*, 2011, **133**, 18042–5.

12 H. Pettersson, T. Gruszecki, L. H. Johansson and P. Johander, *Solar Energy Materials and Solar Cells*, 2003, **77**, 405–413.

13 M. Toivola, T. Peltola, K. Miettunen, J. Halme and P. Lund, *Journal of Nanoscience and Nanotechnology*, 2010, **10**, 1078–1084.

14 A. Mathew, G. Mohan Rao and N. Munichandraiah, *Advanced Materials Letters*, 2014, **5**, 180–183.

15 K. Fredin, E. Johansson, T. Blom, M. Hedlund, K. Leifer and H. Rensmo, *Synthetic Metals*, 2009, **159**, 166–170.

16 M. Shima, M. Isomura, K. I. Wakisaka, K. Murata and M. Tanaka, *Solar Energy Materials and Solar Cells*, 2005, **85**, 167–175.

17 S. R. Raga and F. Fabregat-Santiago, *Physical Chemistry Chemical Physics*, 2013, **15**, 2328.

18 K. Fredin, K. F. Anderson, N. W. Duffy, G. J. Wilson, C. J. Fell, D. P. Hagberg, L. Sun, U. Bach and S. E. Lindquist, *Journal of Physical Chemistry C*, 2009, **113**, 18902–18906.

19 P. Tuyet Nguyen, R. Degn, H. Thai Nguyen and T. Lund, *Solar Energy Materials and Solar Cells*, 2009, **93**, 1939–1945.

20 H. T. Nguyen, H. M. Ta and T. Lund, *Solar Energy Materials and Solar Cells*, 2007, **91**, 1934–1942.

21 D. Bari, N. Wrachien, R. Tagliaferro, S. Penna, T. M. Brown, A. Reale, A. Di Carlo, G. Meneghesso and A. Cester, *Microelectronics Reliability*, 2011, **51**, 1762–1766.

22 Y. Mee Jung, Y. Park, S. Sarker, J.-J. Lee, U. Dembereldorj and S.-W. Joo, *Solar Energy Materials and Solar Cells*, 2011, **95**, 326–331.

23 C. Law, R. Spence and B. C. O'Regan, *Journal of Materials Chemistry A*, 2013, **1**, 14154.

24 M. K. Nazeeruddin, P. Péchy and M. Grätzel, *Chemical Communications*, 1997, **1**, 1705–1706.

25 M. K. Nazeeruddin, S. M. Zakeeruddin, R. Humphry-Baker, M. Jirousek, P. Liska, N. Vlachopoulos, V. Shklover, C.-H. Fischer and M. Grätzel, *Inorganic chemistry*, 1999, **38**, 6298–6305.

26 M. K. Nazeeruddin, R. Humphry-Baker, P. Liska and M. Grätzel, *The Journal of Physical Chemistry B*, 2003, **107**, 8981–8987.

27 M. K. Nazeeruddin, F. De Angelis, S. Fantacci, A. Selloni, G. Viscardi, P. Liska, S. Ito, B. Takeru and M. Grätzel, *J. Am. Chem. Soc.*, 2005, **127**, 16835–16847.

28 A. Mishra, M. Fischer and P. Bäuerle, *Angewandte Chemie International Edition*, 2009, **48**, 2474–2499.

29 W. Zeng, Y. Cao, Y. Bai, Y. Wang, Y. Shi, M. Zhang, F. Wang, C. Pan and P. Wang, *Chemistry of Materials*, 2010, **22**, 1915–1925.

30 D. P. Hagberg, T. Marinado, K. M. Karlsson, K. Nonomura, P. Qin, G. Boschloo, T. Brinck, A. Hagfeldt and L. Sun, *The Journal of Organic Chemistry*, 2007, **72**, 9550–9556.

31 S. M. Feldt, E. A. Gibson, E. Gabrielsson, L. Sun, G. Boschloo and A. Hagfeldt, *Journal of the American Chemical Society*, 2010, **132**, 16714–16724.

32 L. Kloo, *Chemical communications (Cambridge, England)*, 2013, **49**, 6580–3.

33 D. P. Hagberg, X. Jiang, E. Gabrielsson, M. Linder, T. Marinado, T. Brinck, A. Hagfeldt and L. Sun, *Journal of Materials Chemistry*, 2009, **19**, 7232.

34 D. P. Hagberg, T. Edvinsson, T. Marinado, G. Boschloo, A. Hagfeldt and L. Sun, *Chemical communications (Cambridge, England)*, 2006, 2245–2247.

35 D. Kuang, C. Klein, S. Ito, J. E. Moser, R. Humphry-Baker, N. Evans, F. Duriaux, C. Grätzel, S. M. Zakeeruddin and M. Grätzel, *Advanced Materials*, 2007, **19**, 1133–1137.

36 M. K. Nazeeruddin, A. Kay, I. Rodicio, R. Humphry-Baker, E. Mueller, P. Liska, N. Vlachopoulos and M. Graetzel, *Journal of the American Chemical Society*, 1993, **115**, 6382–6390.

37 H. Ellis, S. K. Eriksson, S. M. Feldt, E. Gabrielsson, P. W. Lohse, R. Lindblad and L. Sun, *Journal of Physical Chemistry C*, 2013, **117**, 21029–21036.

38 M. Bässler, J.-O. Forsell, O. Björneholm, R. Feifel, M. Jurvansuu, S. Aksela, S. Sundin, S. Sorensen, R. Nyholm, A. Ausmees and S. Svensson, *Journal of Electron Spectroscopy and Related Phenomena*, 1999, **101-103**, 953–957.

39 M. Bässler, A. Ausmees, M. Jurvansuu, R. Feifel, J.-O. Forsell, P. de Tarso Fonseca, A. Kivimäki, S. Sundin, S. Sorensen, R. Nyholm, O. Björneholm, S. Aksela and S. Svensson, *Nuclear Instruments and Methods in Physics Research Section A: Accelerators, Spectrometers, Detectors and Associated Equipment*, 2001, **469**, 382–393.

40 E. M. J. Johansson, M. Hedlund, H. Siegbahn and H. Rensmo, *Journal of Physical Chemistry B*, 2005, **109**, 22256–22263.

41 G. Boschloo, L. Häggman and A. Hagfeldt, *Journal of Physical Chemistry B*, 2006, **110**, 13144–13150.

42 E. M. J. Johansson, T. Edvinsson, M. Odelius, D. P. Hagberg,

L. Sun, A. Hagfeldt, H. Siegbahn and H. Rensmo, *Journal of Physical Chemistry C*, 2007, **111**, 8580–8586.

43 M. Hahlin, E. M. J. Johansson, S. Plogmaker, M. Odelius, D. P. Hagberg, L. Sun, H. Siegbahn and H. Rensmo, *Physical Chemistry Chemical Physics*, 2010, **12**, 1507–1517.

44 S. K. Eriksson, I. Josefsson, H. Ellis, A. Amat, M. Pastore, J. Oscarsson, R. Lindblad, A. I. K. Eriksson, E. M. J. Johansson, G. Boschloo, A. Hagfeldt, S. Fantacci, M. Odelius and H. Rensmo, *Phys. Chem. Chem. Phys.*, 2016, **18**, 252–260.

45 K. Westermark, S. Tingry, P. Persson, H. Rensmo, S. Lunell, A. Hagfeldt and H. Siegbahn, *Journal of Physical Chemistry B*, 2001, **105**, 7182–7187.

46 J. Nyhlen, G. Boschloo, A. Hagfeldt, L. Kloo and T. Privalov, *Chemphyschem : a European journal of chemical physics and physical chemistry*, 2010, **11**, 1858–62.

47 M. Hahlin, E. M. J. Johansson, R. Schölin, H. Siegbahn and H. Rensmo, *Journal of Physical Chemistry C*, 2011, **115**, 11996–12004.

48 S. Chaturvedi, J. A. Rodriguez, T. Jirsak and J. Hrbek, *The Journal of Physical Chemistry B*, 1998, **102**, 7033–7043.

49 A. Rodriguez, T. Jirsak, S. Chaturvedi and M. Kuhn, *Surface Science*, 1999, **442**, 400–412.

50 J. A. Rodriguez, J. Hrbek, Z. Chang, J. Dvorak, T. Jirsak and A. Maiti, *Physical Review B*, 2002, **65**, 235414.

51 D. Stoltz, A. Onsten, U. O. Karlsson and M. Gothelid, *Applied Physics Letters*, 2007, **91**, 93107.

52 E. M. J. Johansson, M. Odelius, S. Plogmaker, M. Gorgoi, S. Svensson, H. Siegbahn and H. Rensmo, *Journal of Physical Chemistry C*, 2010, **114**, 10314–10322.